Static pressure distribution in the free turbulent jet

By DAVID R. MILLER* and EDWARD W. COMINGS
Purdue University, Lafayette, Indiana

(*Received* 5 *March* 1957)

Summary

Measurements of mean velocity, turbulent stress and static pressure were made in the mixing region of a jet of air issuing from a slot nozzle into still air. The velocity was low and the two-dimensional flow was effectively incompressible. The results are examined in terms of the unsimplified equations of fluid motion, and comparisons are drawn with the common assumptions and simplifications of free jet theory. Appreciable deviations from isobaric conditions exist and the deviations are closely related to the local turbulent stresses. Negative static pressures were encountered everywhere in the mixing field except in the potential wedge region immediately adjacent to the nozzle. Lateral profiles of mean longitudinal velocity conformed closely to an error curve at all stations further than 7 slot widths from the nozzle mouth. An asymptotic approach to complete self-preservation of the flow was observed.

1. Introduction

Few turbulent flows have received more experimental and theoretical study than the simple free jet. Nevertheless, very little appears to be known of the role of the mean static pressure in the jet flow. It is commonly assumed (Alexander *et al.* 1953; Liepmann & Laufer 1947; Pai 1954; Schlichting 1955) that the mean static pressure gradient in the direction of the jet flow is everywhere negligibly small compared to other mean forces on the fluid. Although this assumption seems to be justified in the approximate calculation of mean velocity distributions, a consideration of the departures from it may lead to a better understanding of the structure of the flow.

Pitot tube static-tap pressure measurements have been reported for the coaxial water jet by Viktorin (1941), for the round compressible air jet by Warren (1955), and for incompressible air flows in ducts by Fage (1936) and in two-dimensional wakes by Fage and by Schlichting (1930). These measurements, while revealing significant departures from isobaric flow, were too fragmentary for detailed interpretation in terms of the basic equations of fluid motion.

In this investigation, the static pressure, mean velocity and turbulent stress fields of a two-dimensional, incompressible, free turbulent air jet

* Now at Research and Engineering Division, Monsanto Chemical Company, Dayton, Ohio.

were measured and analysed. The selection of a two-dimensional flow permitted the use of a static pressure probe insensitive to local mean flow direction and turbulent velocity fluctuations in the plane of mean flow. Although mean velocity data have been published for the two-dimensional jet by Förthmann (1934) and by Reichardt (1941), the static pressure and turbulence measurements reported here are believed to be unique.

2. Theory

The geometry of the two-dimensional jet is indicated in figure 1. All solid boundaries, shown in cross-section, are sufficiently extended in the perpendicular z-direction to ensure two-dimensional flow throughout the region of measurement in the plane $z = 0$. Geometrical symmetry of the boundaries requires functional symmetry of all scalar flow variables about the centreplane ($y = 0$).

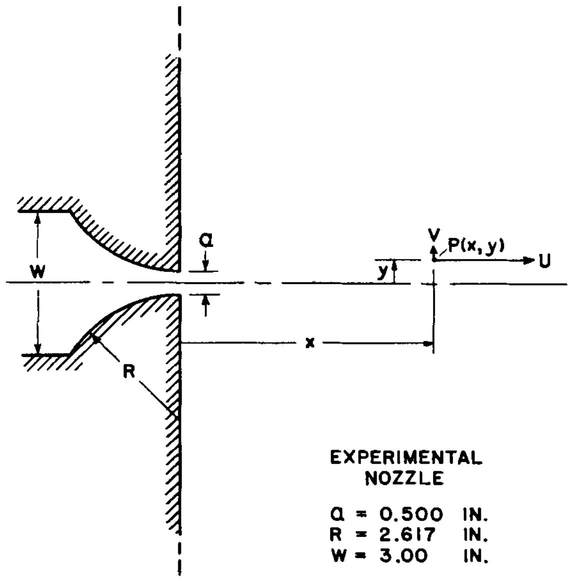

Figure 1. Nozzle and flow geometry.

Equations of motion

Under the restrictions placed on the flow (two-dimensional, incompressible, steady on the average), the appropriate equations of motion, with the customary notation, are:

$$\text{(Continuity)} \quad \frac{\partial U}{\partial x} + \frac{\partial V}{\partial y} = 0, \tag{1}$$

$$(x\text{-Reynolds}) \quad \frac{\partial}{\partial x}(\rho U^2 + \rho\overline{u'^2} + \bar{p}) + \frac{\partial}{\partial y}(\rho UV - \tau + \mu\zeta) = 0, \tag{2}$$

$$(y\text{-Reynolds}) \quad \frac{\partial}{\partial y}(\rho V^2 + \rho\overline{v'^2} + \bar{p}) + \frac{\partial}{\partial x}(\rho UV - \tau - \mu\zeta) = 0, \tag{3}$$

where $\tau = -\rho\overline{u'v'}$ is the turbulent shear stress and $\zeta = \partial V/\partial x - \partial U/\partial y$ is the mean vorticity. Equations (2) and (3) are easily obtained from more common forms of the Reynolds equations given by Goldstein (1938) and by Townsend (1956) with the aid of (1).

Boundary conditions

Those variables which are odd functions of y (V, UV, τ, ζ) are zero at $y = 0$; variables which are even functions in y (U, U^2, V^2, $\overline{u'^2}$, $\overline{v'^2}$, $\bar{p}$), have zero derivatives in the y-direction at $y = 0$. In addition, all variables and their directional derivatives of all orders approach zero as $|y|$ approaches infinity. (In the actual experiment there was a low velocity recirculation of air from the downstream to the upstream portions of the jet and the region of flow was finite in the transverse direction.) It is convenient to define two additional boundaries, $y = \pm\lambda(x)$, outside which the flow is essentially nonturbulent. On and outside these boundaries the turbulent stresses ($\rho\overline{u'^2}$, $\rho\overline{v'^2}$, τ) and their derivatives are zero.

Integral forms of the equations

Making use of the boundary conditions, integration of (1), (2) and (3) in the y-direction gives:

$$\int_0 \frac{\partial U}{\partial x}\, dy + V = 0, \tag{4}$$

$$\int_0 \frac{\partial}{\partial x}(\rho U^2 + \rho\overline{u'^2} + \bar{p})\, dy + \rho UV - \tau + \mu\zeta = 0, \tag{5}$$

$$\int_0 \frac{\partial}{\partial x}(\rho UV - \tau - \mu\zeta)\, dy + \rho V^2 + \rho(\overline{v'^2} - \overline{v_e'^2}) + \bar{p} - \bar{p}_c = 0. \tag{6}$$

In this investigation, dimensionless forms of these three equations were used to calculate the distributions of V, τ and $\overline{v'^2}$ in the fully turbulent region from measured distributions of U, $\overline{u'^2}$ and $\bar{p}$.

Taking infinity as the upper limit in (4) and (5) gives the total mass and momentum flux integrals;

$$\int_0^\infty U\, dy = I \text{ (constant)}, \tag{7}$$

$$\int_0^\infty (\rho U^2 + \rho\overline{u'^2} + \bar{p})\, dy = J \text{ (constant)}. \tag{8}$$

Simplifications used in the theory of fully turbulent flow

Equations (1), (2) and (3) contain six dependent variables, and solutions of the problem cannot, therefore, be obtained by wholly analytic means. A number of simplifications based on experiment, assumption or hypothesis have appeared in the literature, and are described in the remaining part of this section. Heretofore, the lack of sufficiently complete empirical information has prevented a critical evaluation of some of these simplifications, particularly those involving static pressure assumptions.

1. *Reynolds number similarity.* It has been observed by Townsend (1956) that in a fully turbulent flow there exists a region including almost all of the flow in which the direct action of viscosity on the mean flow is negligible, i.e. in which

$$|\rho UV-\tau| \gg |\mu\zeta| \quad \text{for } |y| < \lambda(x). \tag{9}$$

The regions of laminar flow outside the turbulent jet are excluded.

2. *Self-preservation.* Mean velocity measurements in the fully turbulent region of the free jet by Reichardt (1941) reveal that transverse distributions of U retain the same functional form at all downstream locations while changing only in scale, i.e.

$$U = U_c f_1(\eta), \quad \text{where } \eta = y/b. \tag{10}$$

The scale factors U_c (mean velocity on the centreplane) and b (jet width) are functions of x alone. In this investigation b is defined by the relation

$$b(x) = \int_0^\infty (U/U_c)^2\, dy. \tag{11}$$

Townsend (1956) discusses the hypothetical flow wherein all flow variables of equations (1), (2) and (3) (except the vorticity) are self-preserving in the same sense as U, i.e.

$$\overline{u'^2} = U_c^2 f_2(\eta), \text{ etc.} \tag{12}$$

He shows that complete self-preservation is theoretically possible in the two-dimensional free jet and that necessary conditions are:

$$db/dx = c(\text{constant}), \quad \text{or } b = c(x-x_0), \tag{13}$$

and

$$U_c^2 \sim (x-x_0)^{-k}, \tag{14}$$

where k is a constant. Mean velocity measurements in the two-dimensional air jet by Förthmann (1934) and Reichardt (1942), show excellent agreement with these conditions and give values for the constants,

$$c \doteqdot 0{\cdot}075 \quad \text{and } k \doteqdot 1{\cdot}00. \tag{15}$$

However, measurements of turbulent stresses in the round jet by Corrsin (1943) do not exhibit self-preservation within 40 nozzle diameters of the nozzle although a tendency toward self-preservation is apparent. This has led Townsend to conclude that complete self-preservation may be an asymptotic condition not valid over the usual range of measurement. It should be noted that the nonturbulent flow surrounding an actual jet cannot be fully self-preserving.

3. *x-Reynolds equation.* In calculations of mean velocity distributions, it is commonly assumed, as by Pai (1954) and Schlichting (1955), that gradients in the x-direction of the turbulent stress $\rho\overline{u'^2}$ and the mean static pressure are negligible compared to the other forces acting on the mean flow, i.e. that

$$\left|\frac{\partial}{\partial x}(\rho\overline{u'^2}+\bar{p})\right| \ll \left|\frac{\partial}{\partial y}(\rho UV-\tau+\mu\zeta)\right|. \tag{16}$$

When, in addition, the viscous stress is neglected, this assumption leads to simplified forms of the x-Reynolds equation,

$$\frac{\partial}{\partial y}(\rho U^2) + \frac{\partial}{\partial x}(\rho UV - \tau) \doteqdot 0, \tag{17}$$

and of the momentum integral (8),

$$\int_0^\infty \rho U^2\, dy = \rho b U_c^2 \doteqdot J. \tag{18}$$

4. *Hypothetical independent equations.* Self-preserving analytic solutions for U, V and τ can now be obtained when an independent relation between one or more of these variables is assumed. The new relation must be independent of equations (1) and (17), which are also used in the calculation. A number of such solutions (Görtler 1942; Reichardt 1941; Tollmein 1926) have been based on such independent relations as the 'mixing length' hypotheses of Prandtl (1942), Taylor (1938), and von Kármán (1934). Two are presented here for later comparison.

(*a*) Görtler's exchange coefficient

Hypothesis: $\tau = \mu_T(x)\,\dfrac{\partial U}{\partial y}$

Solution for U: $U = U_c \operatorname{sech}^2(\tfrac{2}{3}\eta)$. (19)

(*b*) Reichardt's thermal conduction analogy

Hypothesis: $\dfrac{\partial U^2}{\partial x} = \Lambda(x)\,\dfrac{\partial^2 U^2}{\partial y^2}$

Solution for U: $U = U_c \exp(-\tfrac{1}{8}\pi\eta^2)$. (20)

Several authors (Corrsin 1943, Liepmann & Laufer 1947, and Townsend 1956) have noted the shortcomings of these simple hypotheses.

5. *y-Reynolds equation.* Tollmien (1926) assumed that the turbulent y-stress ($\rho\overline{v'^2}$) is negligible in the y-Reynolds equation, so that

$$\frac{\partial}{\partial y}(\rho V^2 + \bar{p}) + \frac{\partial}{\partial x}(\rho UV - \tau) \doteqdot 0, \tag{21}$$

and then solved for the centreplane static pressure;

$$\bar{p}_c \doteqdot 0{\cdot}263 c^2 \rho U_c^2. \tag{22}$$

Values of U, V and τ needed in the calculation were obtained in the manner of the preceding paragraph using Prandtl's first mixing length hypothesis. Since $c \doteqdot 0{\cdot}075$ in the two-dimensional air jet, he concluded that the static pressure can be neglected in both Reynolds equations. This conclusion is in direct contradiction to a theoretical result described by Townsend (1956). A dimensional analysis of the magnitudes of the various terms in the y-Reynolds equation led Townsend to the conclusion that the lateral gradients of the turbulent y-stress and static pressure are the dominant terms and that the integrated form of the equation may be written

$$\bar{p} + \rho\overline{v'^2} \doteqdot p_\lambda(x), \tag{23}$$

where $p_\lambda(x)$ is a function of x and equals the static pressure 'outside the flow'.

3. Equipment and procedure

Flow system

The flow system is illustrated in figure 2. The nozzle, of aspect ratio 40:1 (20 in. by 0·5 in.), was specially designed for two-dimensional investigations. Control of the turbulence level was provided by two 15 mesh screens and a honeycomb, followed by a two-stage 56:1 contraction in area. The jet emerging from the nozzle was allowed to mix laterally with still air. 'Ceiling' and 'floor' boundaries helped to maintain the two-dimensional character of the jet. All measurements were taken in a plane parallel to and midway between them. The floor consisted of

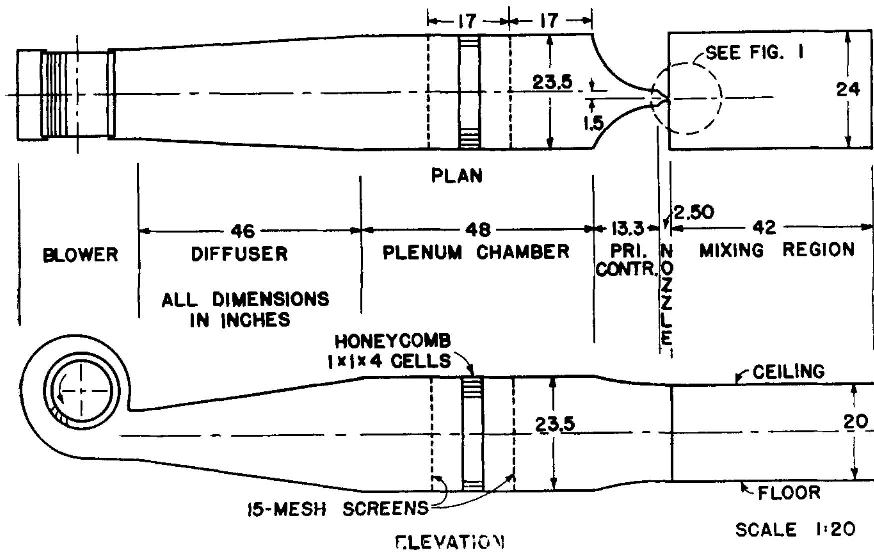

Figure 2. Flow system.

removable plywood sections which provided access for the probes. A lead-screw traversing mechanism, located beneath the floor, supported and positioned the probes. It permitted manual positioning of the probes in the (x, y)-plane with an estimated accuracy of 0·002 in. The centrifugal blower was driven at 750 rpm (except during hot-wire calibration) by a three-phase induction motor. All measurements were made at a nozzle mouth velocity U_r of 72 ft./sec, corresponding to an exit Reynolds number (aU_r/ν) of $1{\cdot}78 \times 10^4$.

Static pressure equipment

Figure 3 shows the design of the static pressure probe. Reflections of the nozzle mouth on the polished surface of the disk were used in aligning the probe accurately in the plane of the flow. All pressure readings were made relative to a reference tap exposed to stagnant atmosphere far from the mixing region. A Prandtl-type micromanometer (Flow Corporation

Model MM-2) was used in all pressure measurements. This instrument has a range of 0–2 in. and an accuracy of $\pm 0{\cdot}0004$ in. of manometer liquid (n-butyl alcohol). No corrections (Fage 1936; Goldstein 1936) were applied to the pressure measurements to account for the effect of the z-velocity fluctuations on the probe pressure. The maximum error in the measurements is estimated to be of the order of 5%. This estimate is based on the assumption of equality of the intensities of the different fluctuation velocity components on the centre-plane of the jet. Equality has been observed on the

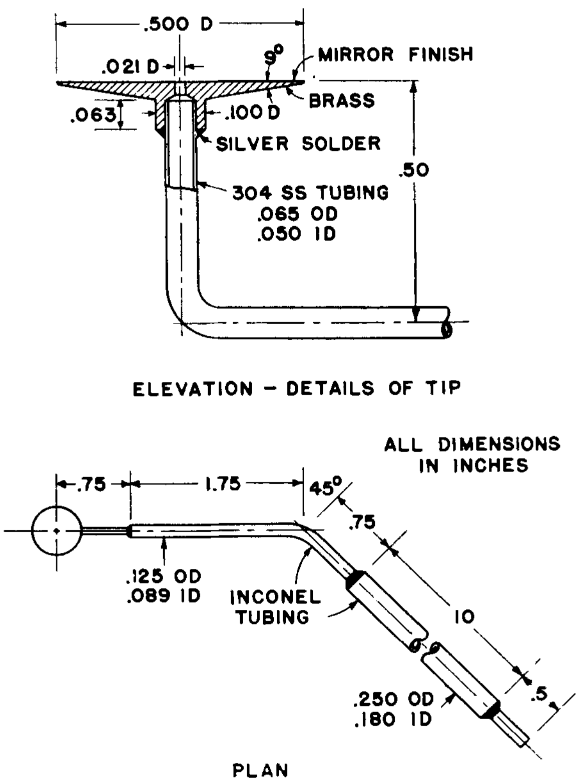

Figure 3. Static pressure probe.

centre-line of a round jet by Corrsin (1943) and on the centre-plane of a two-dimensional wake by Fage (1936). The values of $\overline{v'^2}$ shown in figure 9 were calculated from measurements of $\overline{u'^2}$, U and $\bar{p}$ and were found to approach $\overline{u'^2}$ on the centre-plane at large distances from the nozzle, as would be expected in agreement with the observations of Corrsin and of Fage. The measured $\bar{p}$ is the most important term in this calculation and significant errors in the measurement of the static pressure would be reflected in corresponding deviations from the equality of $\overline{u'^2}$ and $\overline{v'^2}$.

Hot-wire equipment

The hot-wire anemometer constructed for this study was of the constant temperature type and was very similar in design and performance to the anemometer described by Laurence & Landes (1952). A Rubicon potentiometer and an electronic mean-square circuit were used in the measurement of the DC and AC components of the wire heating current. The tungsten hot-wire used to measure both U and $\overline{u'^2}$ had a diameter of 0·0002 in. and an active length of 0·08 in., and was supported in a vertical position in the flow. Mean velocity hot-wire calibrations were carried out before and after each series of hot-wire measurements. An impact tube, mounted in a probe with static taps in opposing parallel walls, was used as the standard of velocity. Simultaneous readings of the velocity head and the wire heating current at two or more velocities constituted a calibration. All calibrations were made in the low-turbulence region at the nozzle mouth. The limiting factor in the accuracy of measurements was the observer's ability to judge the mean value of a randomly fluctuating visual signal. It is estimated that hot-wire mean velocity measurements were subject to a maximum error of $\pm 3\%$ of U_r.

4. Results and discussion

Hot-wire and static pressure traverses, made at 11 lateral stations and along the centre-plane, covered the entire region of turbulent flow out to a distance $40a$ (20 in.) from the nozzle. The measurements, consisting

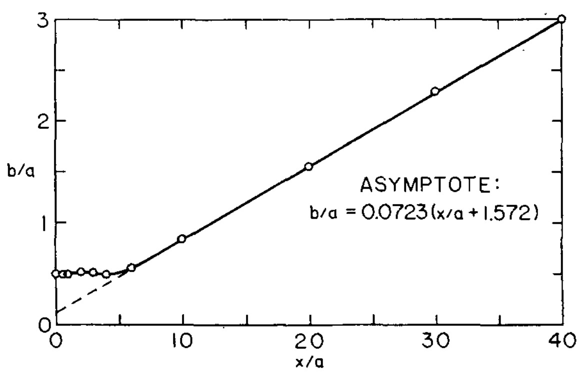

Figure 4. Jet width.

of voltage, current, micrometer and scale readings, were reduced to the usable dimensionless quantities by a digital computer (Electrodata Model 203). All lateral profiles were 'folded' before plotting by averaging computed values on each side of and equidistant from the centre-plane. Only minor asymmetries were apparent in the full profiles.

Figures 4 through 10 present the main experimental results in dimensionless form. Complete tables of data for the single jet reported here and for a double jet system are available elsewhere (Miller 1957). The jet width is shown as a function of downstream position in figure 4. The width is approximately constant for the first four slot widths from the nozzle. Farther downstream, a transition to a linear spread is observed. From $x/a = 7$ to the farthest measurement station, the jet width is well described by equation (13), least-mean-square values of the constants being $c = 0{\cdot}0723$ and $x_0/a = -1{\cdot}572$.

The decay curve for the centreplane velocity (squared) appears in figure 5. The straight portion of the curve for $x/a > 7$ has a slope of $-1{\cdot}028$ as compared to a slope of -1 predicted by the approximate equation (18). The behaviour of b and U_c with distance from the nozzle defines two distinctive flow regimes, the transition flow region extending from the nozzle to $x/a = 7$, and the fully turbulent region lying farther downstream. These two regions are considered separately.

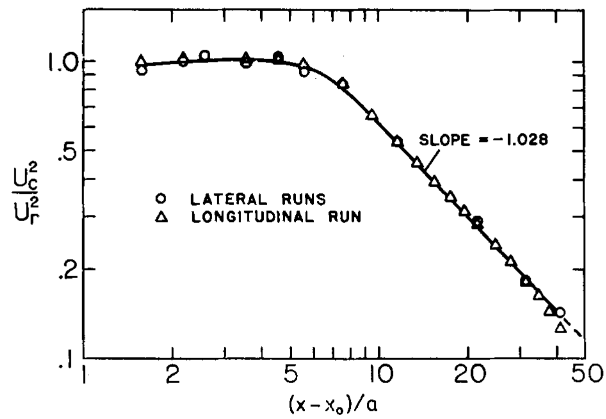

Figure 5. Centreplane velocity decay.

Fully turbulent region

Figure 6 is a composite plot of the U-profiles measured at $x/a = 10, 20, 30$ and 40. In this and other figures pertaining to the fully turbulent region, U_c and b, both functions of x, are used to normalize the data. All experimental points lie on the single curve, within the limit of error, indicating a high degree of self-preservation of the mean velocity profiles. The plotted points in the low velocity region do not represent U truly since the single hot-wire does not distinguish between U and V. The points actually represent $\sqrt{(U^2+V^2)}/U_c$. Making use of this fact and equation (4), the true values of U can be computed. Both the corrected and uncorrected profiles are shown in figure 6, as well as the square of the corrected profile. The smoothed and corrected experimental curve is seen to be in good agreement with points on the error curve of Reichardt's analysis (see (20)). Görtler's profile (see (19)) deviates widely from the data for values of y/b greater than 1·8, indicating that the eddy viscosity is not constant across a section but decreases with distance from the centre-plane.

Turbulent x-stress profiles appear in figure 7. The most striking feature of this plot is the merging of the curves into a single envelope curve in the outer region of mixing. Partial self-preservation is thus exhibited with

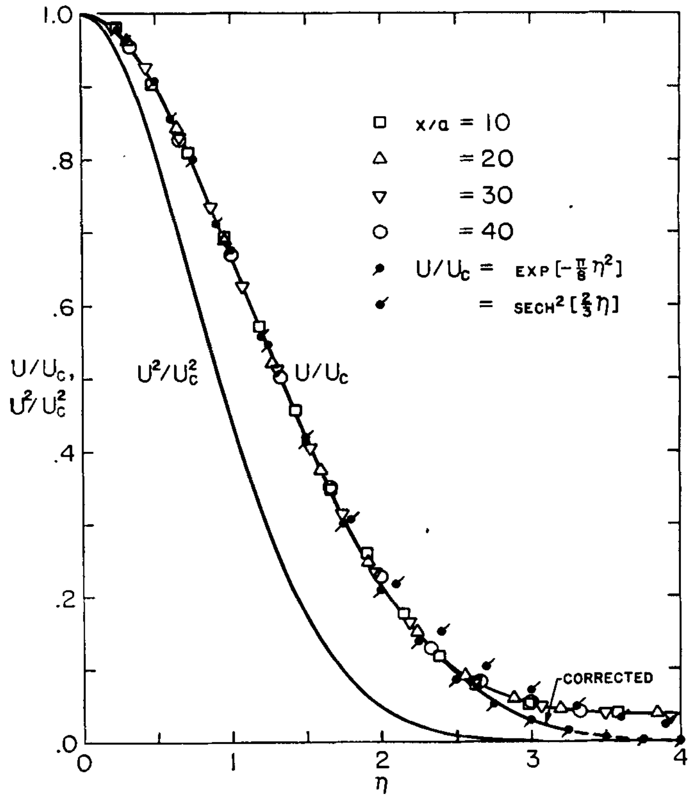

Figure 6. Mean velocity profiles—fully turbulent region.

a definite tendency toward complete self-preservation as the distance from the nozzle increases. Each curve of figure 7 is well correlated by a summation of two error curves. From the trend in the error curve parameters with distance, it is reasonable to expect that the asymptotic profile is approximated by the empirical relation

$$(\overline{u'^2}/U_c^2)_{x=\infty} \doteqdot 0{\cdot}17\exp(-0{\cdot}51\eta^2) - 0{\cdot}10\exp(-1{\cdot}15\eta^2). \tag{24}$$

The outer boundary of turbulence is seen to fall at $y/b \doteqdot 4$, i.e. $\lambda \doteqdot 4b$ in the fully turbulent region.

Static pressure data are plotted in figure 8. The gradual transition of the profile with longitudinal distance is apparent. Partial self-preservation is not observed in these curves. However, the trend in the shape of the curves is toward a stable functional form, varying only in amplitude as the distance from the nozzle increases. The two farthest profiles are well described by the simple error curves

$$[(\bar{p}-\bar{p}_\lambda)/\rho U_c^2]_{x/a=30} \doteqdot -0{\cdot}054\exp(-0{\cdot}30\eta^2), \tag{25 a}$$

$$[(\bar{p}-\bar{p}_\lambda)/\rho U_c^2]_{x/a=40} \doteqdot -0{\cdot}060\exp(-0{\cdot}30\eta^2). \tag{25 b}$$

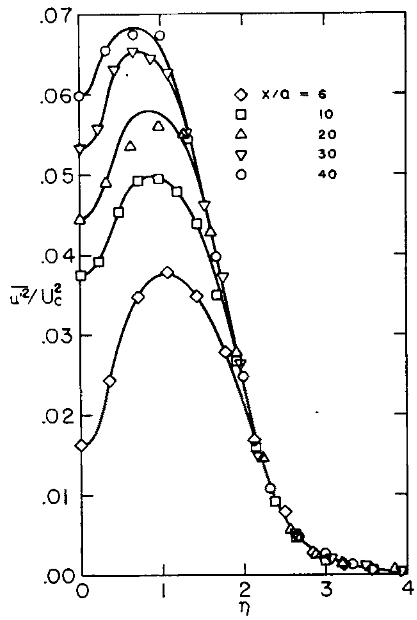

Figure 7. Turbulent x-stress profiles—fully turbulent region.

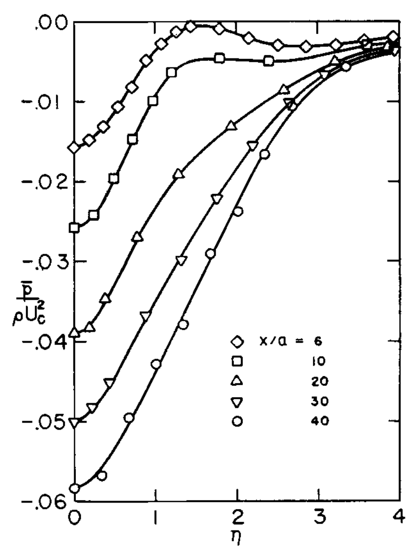

Figure 8. Static pressure profiles—fully turbulent region.

The correspondence is better for the profile at $x/a = 40$, indicating that functional self-preservation is achieved close to this station. Note that $\overline{p}_\lambda$ is neither zero nor constant with x as is sometimes assumed. Because it is not self-preserving, it has been subtracted from $\overline{p}$ in equation (25).

A comparison of the empirical coefficients of equations (25 a, b) with the corresponding centre-plane values of $\overline{u'^2}/U_c^2$ of figure 7 reveals that the quantities are very nearly equal. If it is assumed that this equality persists for larger values of x, the asymptotic solution for the static pressure is

$$[(\bar{p}-\bar{p}_\lambda)/\rho U_c^2]_{x=\infty} \doteqdot -0{\cdot}07\exp(-0{\cdot}30\eta^2), \tag{26}$$

where the coefficient is obtained from equation (24).

Tollmien's solution for the static pressure on the centre-plane (see (22)) gives $\bar{p}_c/\rho U_c^2 = 0{\cdot}00137$ when $c = 0{\cdot}0723$, whereas the measured values are:

$x/a =$	10	20	30	40
$\bar{p}_c/\rho U_c^2 =$	$-0{\cdot}0259$	$-0{\cdot}0389$	$-0{\cdot}0498$	$-0{\cdot}0582$.

The lack of equality indicates that Tollmien's basic assumption (21) is grossly in error.

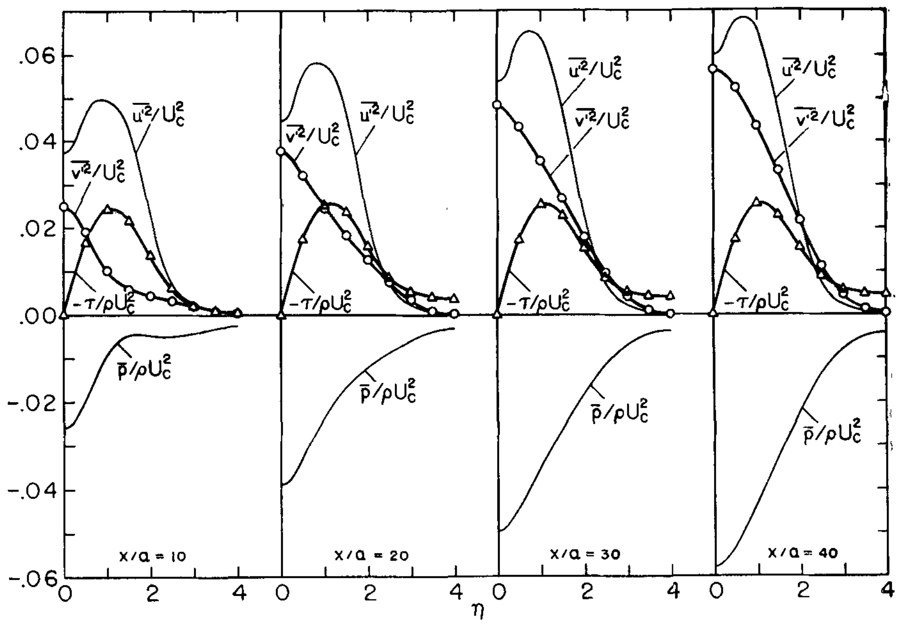

Figure 9. Turbulent y-stress and shearing stress profiles—fully turbulent region.

Using the data of figures 4–8 in equations (4), (5) and (6), values of V, $\overline{v'^2}$ and τ were computed. The latter two variables are plotted in figure 9 together with $\bar{p}$ and $\overline{u'^2}$ for comparison. There is a close negative correspondence, improving with x, between $\bar{p}$ and $\rho\overline{v'^2}$ i.e,.

$$\bar{p}+\rho\overline{v'^2} \doteqdot \bar{p}_\lambda(x). \tag{27}$$

This relation is identical to the one put forward by Townsend (see (23)), and it supplies experimental verification of the validity of his neglect of other terms in the y-Reynolds equation. All remarks made above concerning self-preservation of the static pressure profiles apply also to the turbulent

y-stress profiles. With a change in sign, equations (25 a, b) are equally good descriptions of the $\overline{v'^2}/U_c^2$ profiles. Figure 9 reveals clearly the tendency for $\overline{v'^2}$ to equal $\overline{u'^2}$ on the jet centreplane.

Self-preservation of the turbulent shear stress profiles is seen to exist at $x/a = 20$, 30 and 40. This is to be expected since the other significant terms in equation (5), U^2 and UV, are both fully self-preserving. The fact that these profiles do not approach zero at $y/b = 4$ is taken as an indication of errors of measurement and calculation. The magnitude of the error at the limit of the region of turbulence, where τ should approach zero, is particularly sensitive to the value of k used in the calculation. A value closer to 1·000 than the measured value 1·028 would result in a reduction of the error.

In order to test the assumption underlying equation (16), the values of the two sides of the equation were calculated at a number of different points in the flow and are set out in table 1. The implication of the assumption is that the numbers appearing in the last column of the table should be much less in absolute magnitude than the numbers in the adjoining column. This is seen to be the case at most points; however, there exist isolated regions where the y-derivative passes through zero and the assumption is invalid. Even in these regions equation (17) is not seriously in error,

x/a	y/a	$\frac{a}{\rho U_\tau^2}\frac{\partial}{\partial y}(\rho UV-\tau+\mu\zeta)$	$\frac{a}{\rho U_\tau^2}\frac{\partial}{\partial x}(\rho u'^2+\bar{p})$
10	0	0·048	0·0002
10	1	−0·010	−0·0013
10	2	−0·001	0·0014
10	3	−0·000	0·0001
20	0	0·012	−0·0003
20	1	0·003	−0·0007
20	2	−0·004	−0·0005
20	3	−0·002	0·0007
30	0	0·007	−0·0001
30	1	0·004	−0·0003
30	2	−0·000	−0·0004
30	3	−0·002	−0·0002
40	0	0·003	−0·0000
40	1	0·003	−0·0001
40	2	0·000	−0·0002
40	3	−0·001	−0·0002

Table 1. Test of approximation underlying equation (13).

because of the small magnitude of the neglected terms. This is a fortunate situation, due largely to the fact that $\rho\overline{u'^2}$ and $\bar{p}$ are of the same order of magnitude and of opposite sign. Their sum and its derivatives are consequently much smaller than either term and its derivatives alone. The x-Reynolds equation simplification leading to (16) is thus justified in free jet flow.

Transition region

Lateral distributions of U, $\overline{u'^2}$ and $\bar{p}$ were measured at $x/a = 0$, 0·6, 1, 2, 3, 4 and 6. The computation procedure for obtaining the corresponding distributions of V, $\overline{v'^2}$ and τ was not used because of the relatively large errors involved in calculating derivatives in this region of large gradients.

The region of low turbulence level $(\sqrt{(\overline{u'^2})}/U \leqslant 0{\cdot}05)$ immediately downstream from the nozzle was contained in a wedge whose vertex fell on the centre-plane at $x/a = 2{\cdot}5$ and whose base coincided with the nozzle mouth. A positive static pressure ridge, straddling the centre-plane and decaying rapidly with x, was found within the 'potential wedge'. This ridge is attributed to the persistence of the pressure distribution created within the nozzle.

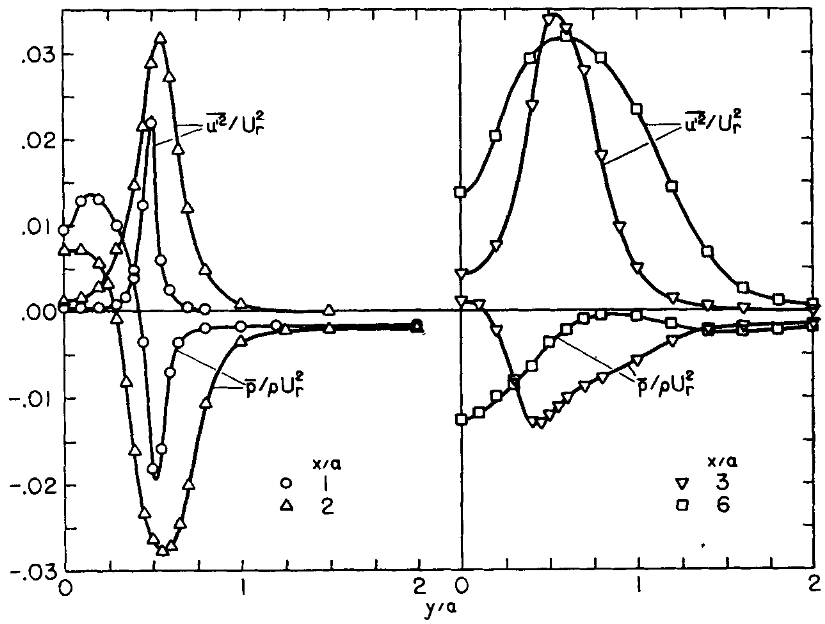

Figure 10. Turbulent x-stress and static pressure profiles—transition region.

Outside the potential wedge, all measured static pressures were negative. Particularly striking were the static pressure trenches appearing on each side of the potential wedge starting at $x/a \doteqdot 0{\cdot}8$ and finally merging at the centreplane at $x/a = 5$. Static pressure measurements reported by Viktorin (1941) and Warren (1955) reveal similar side trenches in the coaxial water jet and round compressible air jet, respectively. Several of the static pressure profiles are plotted in figure 10, the central ridge and side trenches being clearly visible.

The corresponding turbulent x-stress profiles of figure 10 show the development of turbulence in the high shear regions on either side of the potential wedge. Except in the potential wedge, a close negative correspondence is noted between the static pressure and turbulent x-stress profiles at $x/a = 1$ and 2. This correspondence is seen to deteriorate at stations farther downstream.

5. Conclusions

A negative static pressure field exists throughout the turbulent region of the two-dimensional free jet. Its magnitude and directional derivatives are of the same order of magnitude as those of the x and y components of the turbulent stress and the turbulent shear stress.

Static pressure is of minor importance in the x-Reynolds equation of motion for two reasons; (a) the longitudinal mean momentum flux ρU^2 is on the order of 20 times the magnitude of the static pressure, and (b) the longitudinal turbulent stress $\rho\overline{u'^2}$ is of the same order of magnitude as the static pressure but of opposite sign, thereby tending to cancel its influence. The approximation underlying equation (16) is justified despite the fact that it is not correct in certain regions of the flow.

The static pressure $\bar{p}$ and the lateral turbulent stress $\rho\overline{v'^2}$ are the two dominant stresses in the equation of lateral motion in the fully turbulent region. Tollmien's (1926) analysis and conclusions are therefore invalid, whereas Townsend's (1956) analysis is confirmed.

A close correspondence between the static pressure deficiency and turbulent stress components ($\rho\overline{u'^2}$ near the nozzle, $\rho\overline{v'^2}$ in the fully turbulent region) leads to the conclusion that where the flow is turbulent the static pressure deficiency is a manifestation of the presence of turbulence.

Self-preservation of the mean velocity and turbulent shear stress profiles linear spread of the jet, and negligible viscous shear stress, were all observed in the fully turbulent region far from the nozzle, as expected from past work. A tendency toward self-preservation, observed in the static pressure and turbulent stress profiles, supports Townsend's conclusion that complete self-preservation of the flow may be an asymptotic condition not valid over the usual range of observation. The assumption that asymptotic profiles of U, $\overline{v'^2}$, and $\bar{p}$, are simple error curves and that the asymptotic $\overline{u'^2}$ profile is a compound error curve is not inconsistent with the reported data.

Of the various semi-empirical mean velocity solutions, Reichardt's simple error curve describes the data best. The eddy viscosity (or exchange coefficient) is not, therefore, a function of x alone and Görtler's analysis yields a poor representation of the mean-velocity profiles.

The authors wish to express their gratitude for the valuable comments and assistance of Professor Sydney Goldstein of Harvard University and Mr. James C. Laurence of the N.A.C.A. Lewis Flight Propulsion Laboratory. Financial support for this work was generously supplied by The Barrett Division, Allied Chemical and Dye Corporation, and by the Purdue Research Foundation.

References

ALEXANDER, L. G., BARON, T. & COMINGS, E. W. 1953 *University of Illinois, Engineering Experiment Station, Bull. Ser.* no. 413.

CORRSIN, S. 1943 *Nat. Adv. Comm. Aero., Wash., Wartime Rep.* no W-94.

FAGE, A. 1936 *Proc. Roy. Soc.* A, **155**, 576–596.

FÖRTHMANN, E., 1934 *Ing.-Arch.* **5**, 42–54.

GOLDSTEIN, S. 1936 *Proc. Roy. Soc.* A, **155**, 570–575.

GOLDSTEIN, S. (Ed.) *Modern Developments in Fluid Dynamics*, Vol. 1. Oxford Clarendon Press.

GÖRTLER, H. 1942 *Z. angew. Math. Mech.* **22**, 244–254.

KÁRMÁN, T. VON. 1934 *Proc. 4th Int. Congress for Appl. Mech.* 54–91.

LAURENCE, J. C. & LANDES, L. G. 1952 *Nat. Adv. Comm. Aero., Wash., Tech. Note* no. 2843.

LIEPMANN, H. W. & LAUFER, J. 1947 *Nat. Adv. Comm. Aero., Wash., Tech. Note* no. 1257.

MILLER, D. R. 1957 *Ph.D. Dissertation, Purdue University.*

PAI, S.-I. 1954 *Fluid Dynamics of Jets.* Princeton : Van Nostrand.

PRANDTL, L. 1942 *Z. angew Math. Mech.* **22**, 241–243.

REICHARDT, H. 1941 *Z. angew. Math. Mech.* **21**, 257–264.

REICHARDT, H. 1942 *VDI Forschungsheft* 414.

SCHLICHTING, H. 1930 *Ing.-Arch.* **1**, 533.

SCHLICHTING, H. 1955 *Boundary Layer Theory.* New York : McGraw-Hill.

TAYLOR, G. I. 1938 *Proc. 5th Int. Cong. for Appl. Mech.* 294–309.

TOLLMIEN, W. 1926 *Z. angew. Math. Mech.* **6**, 1–12.

TOWNSEND, A. A. 1956 *The Structure of Turbulent Shear Flow.* Cambridge University Press.

VIKTORIN, K. 1941 *Forsch. Geb. Ingen.* **12**, 16–30.

WARREN, W. R. 1955 *J. Aero. Sci.* **22**, 205–207.